

## PROBING PULSAR WINDS WITH GAMMA-RAY BINARIES

Cerutti, B.<sup>1</sup>, Dubus, G.<sup>1</sup> and Henri, G.<sup>1</sup>

### Abstract.

We report on our current studies of high energy radiation from gamma-ray binaries, systems which emit most of their energy above an MeV. Gamma-gamma absorption and anisotropic inverse Compton scattering processes were previously investigated in the context of the young pulsar wind scenario. Here, we report on the gamma-ray emission that would originate from the unshocked pulsar wind itself, instead of originating at the shock between pulsar and stellar wind. The comparison of the theoretical spectral energy distributions with EGRET, HESS and MAGIC observations constrains the particle energy and the shock geometry. The classical pulsar wind model appears incompatible with the data. Alternative models such as the striped pulsar wind may be favored.

### 1 Introduction

Three gamma-ray binaries have been firmly detected in the TeV energy domain: PSR B1259-63 (Aharonian et al. 2005b), LS 5039 (Aharonian et al. 2005a) and LSI +61°303 (Albert et al. 2006). These systems are composed of a massive O/Be type star and a compact object and emit most of their energy above an MeV. A young 48 ms pulsar was detected in PSR B1259-63 (Johnston et al. 1992) but the nature of the compact object in the other two binaries is still undecided. Lack of accretion signs and similarities with PSR B1259-63 favor the presence of a young pulsar (Maraschi & Treves 1981; Martocchia et al. 2005; Dubus 2006b). This hypothesis provides a common scenario to explain the emission from these systems. The gamma-ray emission would be due to particle acceleration at the collision site between the relativistic pulsar wind and the wind of the massive star. Pulsar wind nebula (PWN) of young plerions are known to emit high and very high energy (see the contribution by F. Dubois in this volume). In gamma-ray binaries, the external photon density is high ( $\sim 10^{14}$  ph/cm<sup>3</sup> for LS 5039). An intense gamma-ray flux is expected due to inverse Compton scattering of the stellar photons onto the electrons from the PWN. Because of their tight orbits, gamma-ray radiation can be used to probe the pulsar wind at very small scales (0.01-0.1 AU to be compared with isolated PWN size  $\sim 0.1$  pc). In the classical model of the Crab nebula (Rees & Gunn 1974; Kennel & Coroniti 1984), the pulsar wind nebula is described as being composed of an *unshocked* relativistic cold wind expanding freely until the ram pressure is balanced by the surrounding medium. In the *shocked* region, particles are randomized and accelerated. High energy emission from the shocked pulsar wind was previously investigated for LS 5039 and constraints on the magnetic field, the particle distribution and the total energy injected were formulated at the termination shock (Dubus, Cerutti & Henri 2008). According to the pulsar wind model, high energy emission is expected to originate from the region upstream the shocked region as well. We investigate the theoretical spectral signature from the unshocked pulsar wind in gamma-ray binaries and compare it with observations.

### 2 The unshocked pulsar wind

The rotation of a highly magnetized compact star induces huge electric fields at the surface, sufficiently strong to inject and accelerate electrons and ions into the magnetosphere. Interactions between the magnetic field and the electrons and pair cascading produce a relativistic wind of electrons-positrons, released beyond the light cylinder. The model of plerions PWN describes the unshocked pulsar wind as being isotropic, radial and

---

<sup>1</sup> Laboratoire d'Astrophysique de Grenoble, UMR 5571 CNRS, Université Joseph Fourier, BP 53, 38041 Grenoble, France

monoenergetic with a bulk Lorentz factor  $\gamma_0 \sim 10^6$  far from the light cylinder. The magnetic energy density is assumed to be entirely converted into the kinetic energy of the particles in the wind. The magnetic field is thought to be frozen into the plasma of pairs. Consequently, no synchrotron radiation is expected from this region. However, inverse Compton scattering of stellar photons onto the relativistic electrons is still possible. Previous investigations of the inverse Compton signature from the unshocked pulsar wind were carried out by Bogovalov & Aharonian (2000) for the Crab pulsar and by Ball & Kirk (2000) for the system PSR B1259-63 and found a typical line-like spectrum. Here, we look at the emission from a truncated pulsar wind at a distance  $R_{shock}$  averaged along the orbit for different injected bulk Lorentz factor  $\gamma_0$  in gamma-ray binaries.

### 3 The Compton emission line

#### 3.1 A line-like signature

Because of the relative position of the massive star, the pulsar and the observer, the inverse Compton emission is highly anisotropic. Spectral calculations are based on the anisotropic inverse Compton scattering equations derived in Dubus, Cerutti & Henri (2008). Ultra-relativistic electrons emit most of their radiation in a narrow cone of semi-aperture angle  $1/\gamma_e \ll 1$  due to boosting effects. Assuming the wind expands radially, the observer sees only the emission from the electrons moving toward him. The pulsar wind is observed as a point-like gamma-ray source.

Figure 1 presents computed spectra from a monoenergetic pulsar wind with  $\gamma_0 = 10^5$  applied to LS 5039, taking into account the inverse Compton cooling of the pairs and ignoring gamma-gamma absorption. Spectra present a typical sharp peak at an energy which depends on the bulk Lorentz factor  $\gamma_0$  and whose amplitude on the size of the emitting region  $R_{shock}$ . At the superior conjunction (left panel), Compton cooling is efficient because electron/photon interaction is almost head-on. For small emitting region (orbital separation  $d \gg R_{shock}$ ) the pairs do not have enough time to radiate before reaching the shock, producing less gamma-rays. When the region is extended enough, pairs can cool down efficiently and the amplitude of the spectrum attains a maximum value set by the total injected power into the wind  $L_p$ . Cooled electrons then start to contribute to the low energy tail in the scattered spectrum. Details can be found in Cerutti, Dubus & Henri (2008).

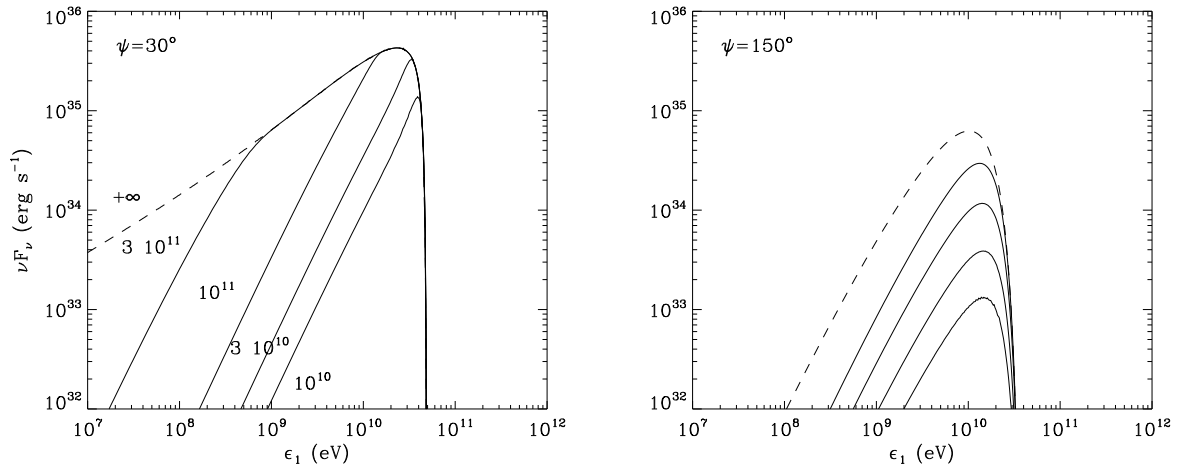


**Fig. 1.** Spectrum from the unshocked pulsar wind applied to LS 5039 with  $\gamma_0 = 10^5$  and  $L_p = 10^{36}$  erg/s. Spectra are calculated at the superior (left panel) and inferior (right panel) conjunctions for different PWN size  $R_{shock} = 10^{10}$  (bottom),  $3 \cdot 10^{10}$ ,  $10^{11}$ ,  $3 \cdot 10^{11}$  cm and  $+\infty$  (dashed line), where  $\psi$  is the viewing angle massive star-pulsar-observer.

#### 3.2 Observational constraints

The intense photon density available in gamma-ray binaries produces a strong line-like signature at every orbital phases in the complete spectral energy distribution. Figure 2 presents computed spectra for LS 5039 averaged

along the orbit, taking into account gamma-gamma absorption calculated in Dubus (2006a). The size of the compact PWN depends on the ratio of the flux wind momentum of the two stars. The orbital parameters and the mass loss rate inferred from optical observations of the massive star suggest a likely size for the nebula of 10% of the orbital separation, assuming a pulsar luminosity of  $L_p = 10^{36}$  erg/s.

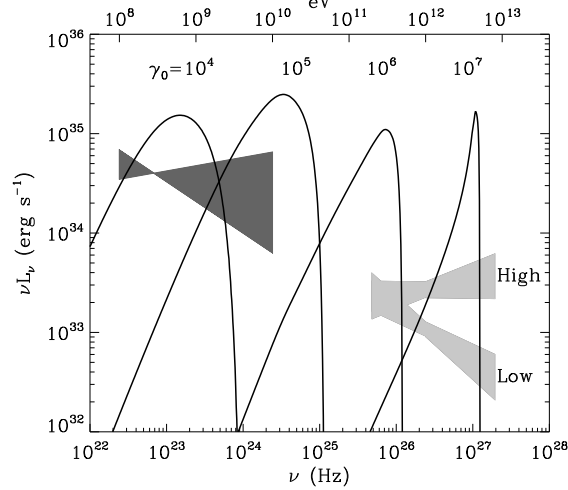


**Fig. 2.** Orbital averaged spectra for LS 5039 and comparison with EGRET (dark bowtie) and HESS (light bowtie) observations. The pulsar luminosity is set at  $L_p = 10^{36}$  erg/s, the nebula size at  $R_{shock}/d = 0.1$  and the bulk Lorentz factor at  $10^4 - 10^7$ .

If we stick to the cold pulsar wind model, the contribution from the unshocked pulsar wind should be a significant contributor to the observed flux. Comparison with EGRET and HESS observations (Hartman et al. 1999; Aharonian et al. 2006) constrains the Lorentz factor to a few  $10^5$  or  $\gamma_0 > 10^7$ . Stronger limits are expected with future GLAST, HESS-2 or CTA measurements.

Several possibilities may reduce this emission to a level consistent with observations. A reduction of the total injected power would diminish the amplitude of the peak. This hypothesis is not viable since it would entail a diminution of the shocked pulsar wind emission as well. A smaller nebula size would also decrease the contribution of the peak but measurements of the stellar wind parameters (McSwain et al. 2004) do not seem to support this possibility. Moreover, a stronger magnetic field would be expected at the collision site, inhibiting the formation of TeV gamma-rays. Another possibility to consider is that the pulsar wind is anisotropic as deduced from X-rays observations of several plerions. A smaller emission is expected if the pulsar has a more pole-on orientation with respect to the observer. The probability to observe the effect of such an anisotropy remains small ( $\sim 5\%$  for each system). Alternatively, the monoenergetic assumption of the unshocked pulsar wind may be incorrect. An injected power-law distribution for the electrons gives spectra difficult to distinguish from the shocked component (e.g. Sierpowska-Bartosik & Torres 2008).

#### 4 The striped wind: a promising alternative?

The *striped wind* is a more realistic model to describe the pulsar wind of an oblique rotator (see the contribution of J. Pétri in this volume). A striped current sheet separates the opposite magnetic field lines originating from the opposite magnetic poles of the neutron star. The alternating magnetic field could be dissipated and accelerate particles close to the equatorial plane. Independently of the dissipation process considered, an upper limit of the Lorentz factor can be formulated based on a causality condition (Arons 2008). Dissipation will occur if the associated timescale  $t_{diss}$  is smaller than the time for a stripe to reach the termination shock region  $t_{flow}$ . The condition  $t_{diss} < t_{flow}$  is fulfilled if  $\Gamma < \sqrt{\beta_{eff} R_{shock}/R_{lc}}$ , where  $\beta_{eff}$  quantifies the efficiency of the dissipation process and  $R_{lc}$  is the radius of the light cylinder. In gamma-ray binaries  $R_{shock}/R_{lc} \sim 10^4$  so that if the bulk Lorentz factor of the pulsar wind  $\Gamma > 100$ , the wind does not have enough time to dissipate. Hence it remains highly magnetized up to the shock, reducing the observational signature of the unshocked wind. Particle-in-cells simulations tend to show that the magnetic energy density is converted into ultra-relativistic particles

at the termination shock (Pétri & Lyubarsky 2007). The conditions in the shocked region seem unchanged compared with the classical picture. Further theoretical and numerical works are necessary to predict accurate observational features from the striped pulsar wind. This model remains a promising alternative to understand the high energy emission from the unshocked pulsar wind in gamma-ray binaries.

## 5 Conclusion

Gamma-ray binaries are particularly interesting objects for the study of pulsar winds at very small scales. The stellar photons act as a probe of the inner structure of pulsar winds. Scattered photons at high energy to the observer betray the physical conditions at the collision site and upstream the termination shock. The study of the emission from the unshocked pulsar wind appears incompatible with the classical model of pulsar wind to the benefit of alternative models such as the striped wind.

## References

- Aharonian, F.A., et al. (HESS collaboration) 2005a, *Science*, 309, 746  
Aharonian, F.A., et al. (HESS collaboration) 2005b, *A&A*, 442, 1  
Aharonian, F.A., et al. (HESS collaboration) 2006, *A&A*, 460, 743  
Albert, J., et al. (MAGIC collaboration) 2006, *Science*, 312, 1771  
Arons, J. 2008, in *40 Years of Pulsars*, ASP Conf. Proc., 983, 200  
Ball, L., & Kirk, J.G. 2000, *Astroparticle Physics*, 12, 335  
Bogovalov, S.V., & Aharonian, F.A. 2000, *MNRAS*, 313, 504  
Cerutti, B., Dubus, G., & Henri, G. 2008, *A&A*, 488, 37  
Dubus, G. 2006a, *A&A*, 451, 9  
Dubus, G. 2006b, *A&A*, 456, 801  
Dubus, G., Cerutti, B., & Henri, G. 2008, *A&A*, 477, 691  
Hartman, R.C., et al. 1999, *ApJS*, 123, 79  
Johnston, S., et al. 1992, *ApJ*, 387, L37  
Kennel, C.F., & Coroniti, F.V. 1984, *ApJ*, 283, 694  
Maraschi, L., & Treves, A. 1981, *MNRAS*, 194, 1L  
Martocchia, A., Motch, C., & Negueruela, I. 2005, *A&A*, 430, 245  
McSwain, M.V., et al. 2004, *ApJ*, 600, 927  
Pétri, J., & Lyubarsky Y.E., 2007, *A&A*, 473, 683  
Rees, M.J., & Gunn, J.E. 1974, *MNRAS*, 167, 1  
Sierpowska-Bartosik, A., & Torres, D.F. 2008, *MNRAS* submitted [arXiv:0801.3427]